Proceedings of the World Congress on Engineering 2013 Vol I,
WCE 2013, July 3 - 5, 2013, London, U.K.

Integral Equations in Cohesive Zones Modelling of Fracture in History Dependent Materials

Layal Hakim, Sergey Mikhailov

***Abstract*—A cohesive zone model of crack propagation in linear visco-elastic materials with non-linear history-dependent rupture criterion is presented. The viscoelaticity is described by a linear Volterra integral operator in time. The stresses on the cohesive zone satisfy the history dependent rupture criterion, given by a non-linear Abel-type integral operator. The crack starts propagating when the crack tip opening reaches a prescribed critical value. A numerical algorithm for computing the evolution of the crack and cohesive zone in time is discussed along with some numerical results.**

***Index Terms*—Keywords: Abel integral equation, viscoelsticity, cohesive zone, history dependent fracture, nonlinear fracture**

I. Introduction

THE cohesive zone, CZ, in a material is the area between two separating but still sufficiently close surfaces ahead of the crack tip, see the shaded region in Figure 1. The cohesive forces present at the cohesive zones pull the cohesive zone faces together. The external load applied to the body, on the contrary, causes the crack faces and CZ faces to move further apart and the crack to propagate.

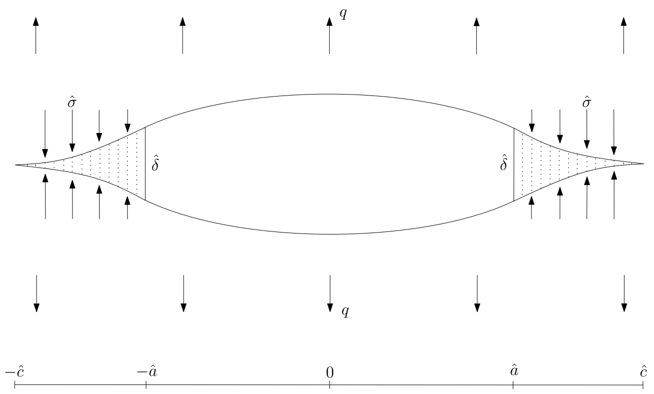

Fig. 1. Cohesive zone

Our aim is to find the time evolution of the CZ before the crack starts propagating, the delay time, after which the crack will start to propagate, and further time evolution of the crack and the CZ. When the crack propagates, the cohesive forces vanish at the points where the cohesive zone opening reaches a critical value and these points become the crack surface points, while the new material points, where the history-dependent normalised equivalent stress reaches a critical value, join the cohesive zone. So, the CZ is practically attached to the crack tip ahead of the crack and moves with the crack, keeping the normalised equivalent stress finite in the body.

One of the most popular CZ models for elasto-perfectly plastic materials is the Dugdale-Leonov-Panasyuk (DLP) (1959-1960) model, see [1], [2]. In the DLP model, the maximal normal stress in the cohesive zones is constant and equals to the material yield stress, $\sigma = \sigma_y$. This model, and several of its modifications, have been widely used in nonlinear fracture mechanics. Another popular CZ model is the Barenblatt (1962) model.

The 3 main components needed to implement CZ models of the DLP-type are: (i) the constitutive equations in the bulk of the material; (ii) the constitutive equations in the cohesive zone; (iii) the criteria for the cohesive zone to break and the crack to propagate.

II. Problem Formulation

The model presented in this paper is an extension of the DLP model to linear visco-elastic materials with non-linear history-dependent constitutive equations in the cohesive zone. To this end, we will replace the DLP cohesive zone stress condition, $\sigma = \sigma_y$, with the condition

$$\underline{\Lambda}(\hat{\boldsymbol{\sigma}};\hat{t}) = 1, \tag{1}$$

where

$$\underline{\Lambda}(\hat{\boldsymbol{\sigma}};\hat{t}) = \left(\frac{\beta}{b\sigma_0^{\beta}}\int_0^{\hat{t}} |\hat{\boldsymbol{\sigma}}(\hat{\tau})|^{\beta}(\hat{t}-\hat{\tau})^{\frac{\beta}{b}-1}d\hat{\tau}\right)^{\frac{1}{\beta}} \tag{2}$$

is the normalised history-dependent equivalent stress, $|\hat{\boldsymbol{\sigma}}|$ is the maximum of the principal stresses, and $\hat{t}$ denotes time. The parameters σ_0 and b are material constants in the assumed power-type relation

$$\hat{t}_\infty(\hat{\sigma}) = \left(\frac{\hat{\sigma}}{\sigma_0}\right)^{-b}$$

between the rupture time $\hat{t}_\infty(\hat{\sigma})$ and the constant uniaxial tensile stress applied to a body without cracks. The parameter β is a material constant in the nonlinear accumulation rule for durability under variable load, see [3].

Note that relations (1)-(2) were implemented in [4] and [5] to solve a similar crack propagation problem without cohesive zone; i.e. it was assumed that when condition (1) is reached at a point, this point becomes part of the crack. However, such approach appeared to be inapplicable for $b \geq 2$. In this paper, a cohesive zone approach is developed instead, in order to cover the larger range of b values relevant to structural materials. In the CZ approach, when condition (1) is reached at a point, this point becomes part of the cohesive zone.

Let the problem geometry be as in Figure 1, i.e, the crack occupies the interval $[-\hat{a}(\hat{t}), \hat{a}(\hat{t})]$ and the cohesive zone

Manuscript received 6th of March, 2013; revised 31st of March, 2013. Details of authors: Both authors are currently at the Department of Mathematical Sciences in Brunel university London, UK; emails: layal.hakim@brunel.ac.uk; sergey.mikhailov@brunel.ac.uk

occupies the intervals $[-\hat{c}(\hat{t}), -\hat{a}(\hat{t})]$ and $[\hat{a}(\hat{t}), \hat{c}(\hat{t})]$ in an infinite plane loaded at infinity by traction $\hat{q}$ in the direction normal to the crack, which is constant in $\hat{x}$, applied at the time $\hat{t} = 0$ and kept constant in time thereafter. The initial CZ tip coordinate and crack tip coordinate are prescribed, $\hat{c}(0) = \hat{a}(0) = \hat{a}_0$, while the functions $\hat{c}(\hat{t})$ and $\hat{a}(\hat{t})$ for time $\hat{t} > 0$ are to be found.

The cohesive zone condition (1)-(2) at a point $\hat{x}$ on the cohesive zone can be rewritten as

$$\int_{\hat{t}_c(\hat{x})}^{\hat{t}} \frac{\hat{\sigma}^\beta(\hat{x},\hat{\tau})}{(\hat{t}-\hat{\tau})^{1-\frac{\beta}{b}}} d\hat{\tau} = \frac{b\sigma_0^\beta}{\beta} - \int_0^{\hat{t}_c(\hat{x})} \frac{\hat{\sigma}^\beta(\hat{x},\hat{\tau})}{(\hat{t}-\hat{\tau})^{1-\frac{\beta}{b}}} d\hat{\tau}, \quad (3)$$

for $\hat{t} \geq \hat{t}_c(\hat{x})$ and $\hat{a}(\hat{t}) \leq |\hat{x}| \leq \hat{c}(\hat{t})$.

Here, $\hat{t}_c(\hat{x})$ denotes the time when the point $\hat{x}$ becomes part of the cohesive zone. Equation (3) is an inhomogeneous nonlinear Volterra integral equation of the Abel type with unknown function $\hat{\sigma}(\hat{x},\hat{t})$ for $\hat{t} \geq \hat{t}_c(\hat{x})$.

We will first consider the case when the bulk of the material is linearly elastic and then convert the obtained solution to the case of linear visco-elastic materials using the so-called Volterra principle. Applying the results by Muskhelishvili (see [6], Section 120), we have for the stresses ahead of the cohesive zone in the elastic material,

$$\hat{\sigma}(\hat{x},\hat{t}) = \frac{\hat{x}}{\sqrt{\hat{x}^2 - \hat{c}^2(\hat{t})}} \left[\hat{q} - \frac{2}{\pi} \int_{\hat{a}(\hat{t})}^{\hat{c}(\hat{t})} \frac{\sqrt{\hat{c}^2(\hat{t}) - \hat{\xi}^2}}{\hat{x}^2 - \hat{\xi}^2} \hat{\sigma}(\hat{\xi},\hat{t}) d\hat{\xi} \right], \quad (4)$$

for $\hat{t} \leq \hat{t}_c(\hat{x})$ and $|\hat{x}| > \hat{c}(\hat{t})$. As one can see from (4), $\hat{\sigma}(\hat{x},\hat{t})$ has generally a square root singularity as $\hat{x}$ tends to $\hat{c}$.

A sufficient condition for the normalised equivalent stress, Λ, to be bounded at the cohesive zone tip is that the stress intensity factor, $\hat{K}$, is zero at the cohesive zone tip. Multiplying the stress in equation (4) by $\sqrt{\hat{x} - \hat{c}(\hat{t})}$ and taking the limit as $\hat{x}$ tends to $\hat{c}(\hat{t})$ yields

$$\hat{K}(\hat{t}) = \sqrt{\frac{\hat{c}(\hat{t})}{2}} \left[\hat{q} - \frac{2}{\pi} \int_{\hat{a}(\hat{t})}^{\hat{c}(\hat{t})} \frac{\hat{\sigma}(\hat{\xi},\hat{t})}{\sqrt{\hat{c}^2(\hat{t}) - \hat{\xi}^2}} d\hat{\xi} \right].$$

To simplify the equations, we will employ the normalisations

$$t = \frac{\hat{t}}{\hat{t}_\infty}, \quad x = \frac{\hat{x}}{\hat{a}_0}, \quad a(t) = \frac{\hat{a}(t\,\hat{t}_\infty)}{\hat{a}_0},$$
$$c(t) = \frac{\hat{c}(t\,\hat{t}_\infty)}{\hat{a}_0}, \quad \sigma(x,t) = \frac{\hat{\sigma}(x\,\hat{a}_0, t\,\hat{t}_\infty)}{\hat{q}},$$
$$K(c,t) = \frac{\hat{K}(c\,\hat{a}_0, t\,\hat{t}_\infty)}{\hat{q}\sqrt{\hat{a}_0}}. \quad (5)$$

Here $\hat{t}_\infty = \hat{t}_\infty(\hat{q}) = \left(\frac{\hat{q}}{\sigma_0}\right)^{-b}$ denotes the fracture time for an infinite plane without a crack under the same load, $\hat{q}$.

Thus, after the normalisation, we state the following principle equations for the considered problem:
(a) the cohesive zone condition (1) in the form

$$\int_{t_c(x)}^{t} \frac{\sigma(x,\tau)^\beta}{(t-\tau)^{1-\frac{\beta}{b}}} d\tau = \frac{b}{\beta} - \int_0^{t_c(x)} \frac{\sigma^\beta(x,\tau)}{(t-\tau)^{1-\frac{\beta}{b}}} d\tau \quad (6)$$

for $a(t) \leq |x| \leq c(t)$;

(b) the expression for the stress ahead of the cohesive zone:

$$\sigma(x,t) = \frac{x}{\sqrt{x^2 - c^2(t)}} \cdot \left(1 - \frac{2}{\pi} \int_{a(t)}^{c(t)} \frac{\sqrt{c^2(t) - \xi^2}}{x^2 - \xi^2} \sigma(\xi,t) d\xi \right) \text{ for } |x| > c(t); \quad (7)$$

(c) the zero stress intensity factor, $K(c,t) = 0$, where

$$K(c,t) = \frac{\sqrt{c(t)}}{\sqrt{2}} - \frac{\sqrt{2c(t)}}{\pi} \int_{a(t)}^{c(t)} \frac{\sigma(\xi,t)}{\sqrt{c^2(t) - \xi^2}} d\xi. \quad (8)$$

III. Cohesive Zone Growth for a Stationary Crack

In this section we will consider the stationary stage, before the crack starts propagating, i.e., $a(t) = a(0) = 1$, and thus only the cohesive zone grows with time. Our aim is to find the cohesive zone tip position $c(t)$ and the crack tip opening.

A. Numerical Method

Let us introduce a time mesh with nodes $t_i = ih$, for $i = 0, 1, 2, 3, ...n$, where h is the time-step size. At each time step t_i, we use the secant method to find the roots, $c(t_i) = c_i$, of the equation $K(c_i, t_i) = 0$, as follows:

1) Take 2 initial approximations, $(c_i)_1$ and $(c_i)_2$, for $c(t_i)$.
2) Obtain $K_1 = K((c_i)_1, t_i)$ and $K_2 = K((c_i)_2, t_i)$ using equation (8). Note that:
   - In order to evaluate the integral in (8),

$$\int_{a(0)}^{c(t_i)} \frac{1}{\sqrt{c^2(t_i) - \xi^2}} \sigma(\xi, t_i) d\xi, \quad (9)$$

   we linearly interpolate $\sigma(\xi, t_i)$ on the cohesive zone between $\xi = c(t_k)$ and $\xi = c(t_{k+1})$, where $k = 0, 1, 2, ...i-1$.
   - On the other hand, to find $\sigma(\xi, t_i)$, at each $\xi = c(t_k)$, we use the Abel integral equation (6). First, we evaluate the integral

$$\int_0^{t_k} \sigma^\beta(c(t_k),\tau)(t-\tau)^{\frac{\beta}{b}-1} d\tau$$

   in the right hand side of equation (6) by piecewise linearly interpolating the function $\sigma^\beta(c(t_k),\tau)$ between $\tau = t_j$ and $\tau = t_{j+1}$ for $j = 0, 1, 2, ...k-1$. Then we use the analytical solution of a generalised Abel type integral equation to solve the integral equation (6).
   - To this end, in turn, we need to find $\sigma^\beta(c(t_k), t_j)$ for $t_j < t_k$ from equation (7) (since $c(t_k) > c(t_j)$), where the integral

$$\int_{a(0)}^{c(t_j)} \frac{\sqrt{c^2(t) - \xi^2}}{c(t_k)^2 - \xi^2} \sigma(\xi, t_j) d\xi$$

   is calculated similarly to integral (9). This means we piecewise linearly interpolate $\sigma(\xi, t_j)$ between $\xi = c(t_m)$ and $\xi = c(t_{m+1})$ for $m = 0, 1, ...j-1$.
3) Find the next approximation for c_i using

$$(c_i)_3 = \frac{K_2(c_i)_1 - K_1(c_i)_2}{K_2 - K_1}$$

ISBN: 978-988-19251-0-7
ISSN: 2078-0958 (Print); ISSN: 2078-0966 (Online)

4) If $|(c_i)_3 - (c_i)_1| < \epsilon$ or $|(c_i)_3 - (c_i)_2| < \epsilon$ allocate $c(t_i) = c_3$ and go to the step $t = t_{i+1}$; otherwise, go to the next item. Here ϵ is some tolerance.
5) Taking the new $(c_i)_2$ as $(c_i)_3$ return to item 2 until convergence is reached.

We have used $\varepsilon = 10^{-8}$ as the tolerance value. All programming was implemented in MATLAB. Using this scheme, we obtained the evolution of the cohesive zone tip position as well as the stress distribution on the cohesive zone.

B. Numerical Results

The graphs presented in Fig. 2 show the results obtained for a stationary crack with $b = 4$ and $\beta = b/2 = 2$ for various mesh sizes.

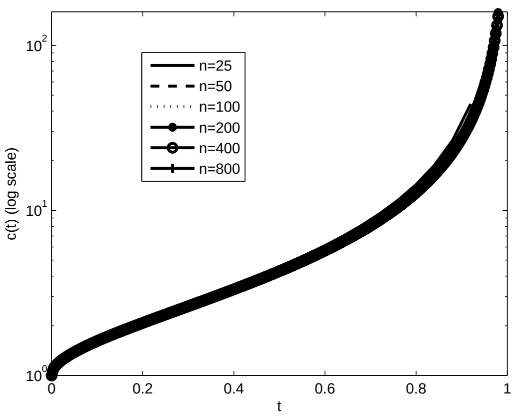

Fig. 2. CZ tip position vs time for $b = 4$, $\beta = 2$, and different meshes

The graph in Fig. 3 is a closer look at the graphs in Fig. 2.

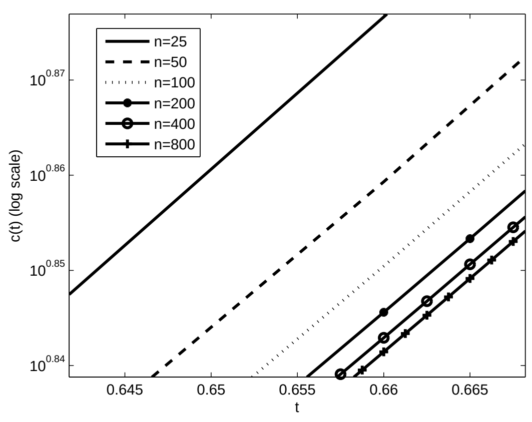

Fig. 3. CZ tip position vs time for $b = 4$, $\beta = 2$ and different meshes, zoomed

The graphs in Figs. 4 and 5 show the results obtained for 3 different values of the parameter β.

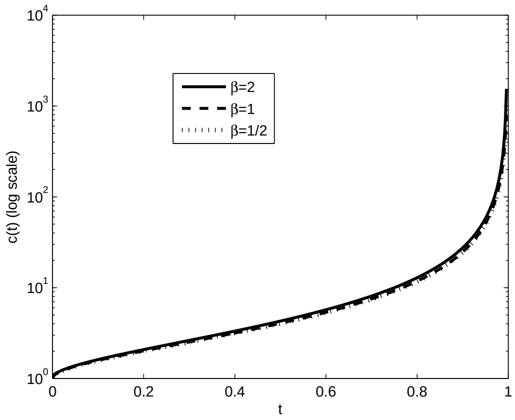

Fig. 4. CZ tip position vs time for $b = 4$ and different β (non-propagating crack)

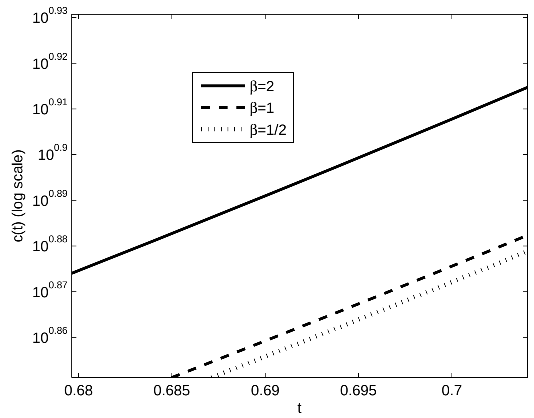

Fig. 5. CZ tip position vs time for $b = 4$ and different β (non-propagating crack), zoomed

Figure 6 shows the stress behaviour with respect to time at the point $x = c(0.6)$, i.e., $t_c(x) = 0.6$.

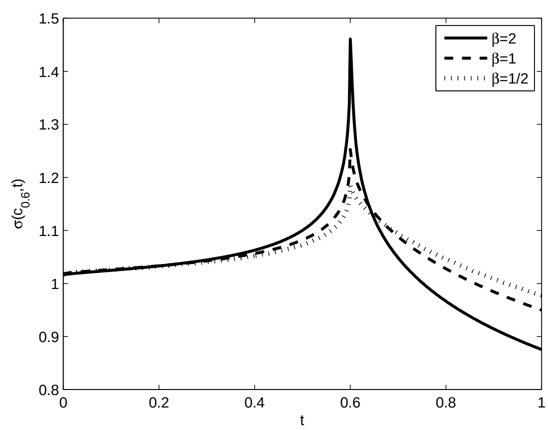

Fig. 6. The stress $\sigma(c(0.6), t)$ vs time for $b = 4$, $n = 500$

C. Crack Tip Opening in the Elastic Case

Using the representations by Muskhelishvili (see [6], Section 120), it can be deduced that the normal displacement

ISBN: 978-988-19251-0-7
ISSN: 2078-0958 (Print); ISSN: 2078-0966 (Online)

jump at a crack+CZ shore point $\hat{x}$ is

$$[\hat{u}_e(\hat{x},\hat{t})] = [\hat{u}_e^{(q)}(\hat{x},\hat{t})] + [\hat{u}_e^{(\sigma)}(\hat{x},\hat{t})]$$

where

$$[\hat{u}_e^{(q)}(\hat{x},\hat{t})] = \frac{4\hat{q}(1-\nu^2)}{E_0}\sqrt{\hat{c}(\hat{t})^2 - \hat{x}^2},$$

$$[\hat{u}_e^{(\sigma)}(\hat{x},\hat{t})] = \frac{4(1-\nu^2)}{\pi E_0}\left(\int_{\hat{a}(\hat{t})}^{\hat{c}(\hat{t})} \sigma(\hat{\xi},\hat{t})\Gamma(\hat{x},\hat{\xi};\hat{c}(\hat{t}))d\hat{\xi}\right),$$

$$\Gamma(\hat{x},\hat{\xi};\hat{c}) = \ln\left[\frac{2\hat{c}^2 - \hat{\xi}^2 - \hat{x}^2 - 2\sqrt{(\hat{c}^2-\hat{x}^2)(\hat{c}^2-\hat{\xi}^2)}}{2\hat{c}^2 - \hat{\xi}^2 - \hat{x}^2 + 2\sqrt{(\hat{c}^2-\hat{x}^2)(\hat{c}^2-\hat{\xi}^2)}}\right].$$

In the above expressions, E_0 and ν denote Young's modulus of elasticity and Poisson's ratio, respectively. We denote the displacement jump at the crack tip, $\hat{x} = \hat{a}$, for the elastic material by

$$\hat{\delta}_e(\hat{t}) := [\hat{u}_e(\hat{a}(\hat{t}),\hat{t})] = \frac{(1-\nu^2)}{E_0}\left(4\hat{q}\sqrt{\hat{c}^2(\hat{t}) - \hat{a}^2(\hat{t})} + \frac{4}{\pi}\int_{\hat{a}(\hat{t})}^{\hat{c}(\hat{t})} \hat{\sigma}(\hat{\xi},\hat{t})\Gamma(\hat{a}(\hat{t}),\hat{\xi},\hat{c}(\hat{t}))d\hat{\xi}\right). \quad (10)$$

and call it the crack tip opening. Using the normalisation

$$[u_e(x,t)] = \frac{E_0[\hat{u}_e\left(\hat{x}\,\hat{a}_0, t\hat{t}_\infty\right)]}{\hat{a}_0\hat{q}\,(1-\nu^2)},\ \delta_e(t) = \frac{E_0\hat{\delta}(t\,\hat{t}_\infty)}{\hat{a}_0\hat{q}(1-\nu^2)}, \quad (11)$$

we obtain

$$[u_e(x,t)] = 4\sqrt{c^2(t) - x^2} + \frac{4}{\pi}\int_{a(t)}^{c(t)} \sigma(\xi,t)\Gamma(x,\xi;c(t))d\xi, \quad (12)$$

$$\delta_e(t) = [u_e(a(t),t)].$$

D. Crack Tip Opening in the Viscoelastic Case

To obtain the crack tip opening in the visco-elastic case, we will implement the so-called Volterra principle, according to which we have to replace the elastic constants E_0 and ν in the elastic solution by the corresponding viscoelastic operators, to arrive at the viscoelastic solution. Although this approach does not always bring a viscoelastic solution for the problems with moving boundaries, it is possible to show, cf. [7], that this approach leads to a viscoelastic solution for the plane symmetric problems with a straight propagating crack. This means that for the viscoelastic problem we can directly use the results by Muskhelishvili for the stress representation given in equation (4) since they do not include the elastic constants at all. For simplicity, we will consider the viscoelastic material with constant (purely elastic) Poisson's ratio. Then, to obtain the crack opening in the viscoelastic case, we have to replace $1/E_0$ in (10) by the second kind Volterra integral operator $\mathbf{E}^{-1}$ defined as

$$\left(\mathbf{E}^{-1}\hat{\sigma}\right)(\hat{t}) = \frac{\hat{\sigma}(\hat{t})}{E_0} - \int_0^{\hat{t}} \dot{J}\left(\hat{t}-\hat{\tau}\right)\sigma(\hat{\tau})\,d\hat{\tau},$$

where the creep function J is known and $\dot{J}$ is its derivative. Hence the viscoelastic crack tip opening becomes

$$\hat{\delta}_v(\hat{t}) = [\hat{u}_v(\hat{a}(\hat{t}),\hat{t})] = \left(\mathbf{E}^{-1}E_0[\hat{u}_e(\hat{a}(\hat{t}),\cdot)]\right)(\hat{t}) = \left(\hat{\delta}_e(\hat{t}) - E_0\int_0^{\hat{t}} \dot{J}\left(\hat{t}-\hat{\tau}\right)[\hat{u}_e(\hat{a}(\hat{t}),\hat{\tau})]d\hat{\tau}\right). \quad (13)$$

In our numerical examples we use the creep function of a standard linear solid (of the Kelvin-Voigt type), namely

$$J\left(\hat{t}-\hat{\tau}\right) = \frac{1}{E_0} + \frac{1}{E_1}\left(1 - e^{-\frac{E_1}{\eta}(\hat{t}-\hat{\tau})}\right), \quad (14)$$
$$\dot{J}\left(\hat{t}-\hat{\tau}\right) = -\frac{1}{\eta}e^{-\frac{E_1}{\eta}(\hat{t}-\hat{\tau})}.$$

Here, η and E_1 are material constants, η/E_1 being the relaxation time and η the viscosity of the polymer. Such viscoelastic models satisfactorily model some polymers, e.g. PMMA (also known as plexiglas).

For J in the form (14), equation (13) becomes

$$\hat{\delta}_v(\hat{t}) = [\hat{u}_v(\hat{a}(\hat{t}),\hat{t})] = \left(\hat{\delta}_e(\hat{t}) + \frac{E_0}{\eta}\int_0^{\hat{t}} e^{-\frac{E_1}{\eta}(\hat{t}-\hat{\tau})}[\hat{u}_e(\hat{a}(\hat{t}),\hat{\tau})]d\hat{\tau}\right). \quad (15)$$

Employing the normalised parameters

$$\delta_v(t) = \frac{E_0\hat{\delta}_v\left(t\hat{t}_\infty\right)}{\hat{a}_0\hat{q}\,(1-\nu^2)},\ A_0 = \frac{E_0\hat{t}_\infty}{\eta},\ A_1 = \frac{E_1\hat{t}_\infty}{\eta}, \quad (16)$$

equation (15) reduces to the following expression for the normalised crack tip opening in the viscoelastic case,

$$\delta_v(t) = [u_v(a(t),t)] = \left(\delta_e(t) + A_0\int_{t_c(a(t))}^{t} e^{-A_1(t-\tau)}[u_e(a(t),\tau)]d\tau\right), \quad (17)$$

where the lower limit of the integral is replaced with $t_c(a(t))$ since $[u_e(x,\tau)] = 0$ when $\tau \le t_c(x)$.

In the numerical examples we used values $A_0 = 2.8695$ and $A_1 = 1.5736$. The graphs in Figs. 7-9 show the stationary crack tip opening evolution for $b = 4$ and different β in the elastic and viscoelastic cases.

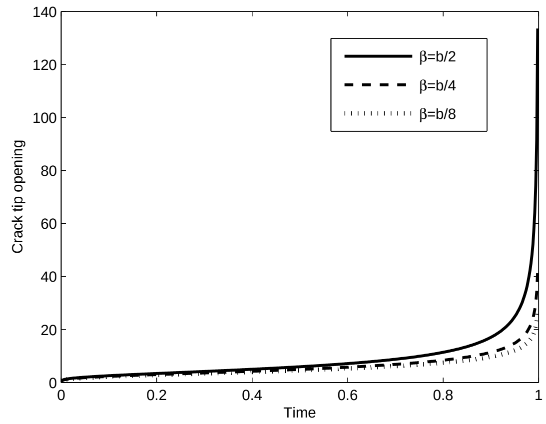

Fig. 7. Crack tip opening vs time for $b = 4$, elastic case

ISBN: 978-988-19251-0-7
ISSN: 2078-0958 (Print); ISSN: 2078-0966 (Online)

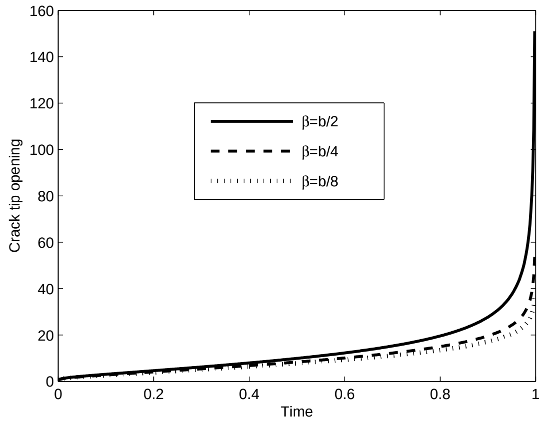

Fig. 8. Crack tip opening vs time for $b = 4$, viscoelastic case

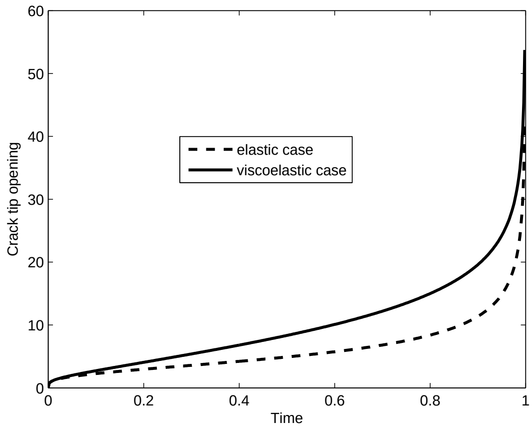

Fig. 9. Crack tip opening vs time for $b = 4$, $\beta = 1$

IV. Crack Propagation

We have, so far, assumed that the crack is stationary and only the cohesive zone is growing ahead of the crack. However, the crack will start to propagate when the crack tip opening $\hat{\delta}$ reaches a critical value $\hat{\delta}_c$, where $\hat{\delta}_c$ is considered as a material constant. The crack and cohesive zone will not necessarily grow at the same rate. The time instant, when the crack tip opening reaches a critical value, will be referred to as the fracture delay time and denoted by $\hat{t}_d$.

Similar to (5), (11) and (16), we employ the following normalised parameters,

$$t_d = \frac{\hat{t}_d}{\hat{t}_\infty}, \quad \delta_c = \frac{\hat{\delta}_c E_0}{\hat{a}_0 \hat{q}(1-\nu^2)}. \tag{18}$$

The aim now is to find t_d, the crack tip coordinate $a(t)$ and the CZ tip coordinate $c(t)$ for $t > t_d$.

A. Numerical Method

Considering uniformly spaced time steps, the crack tip opening $\delta(t_i)$ satisfies equation

$$\delta_e(t_i) = \delta_c, \quad t_i \geq t_d. \tag{19}$$

for the purely elastic case and equation

$$\delta_v(t_i) = \delta_c, \quad t_i \geq t_d. \tag{20}$$

for the viscoelastic case, where $\delta_v(t_i)$ is given by (17).

We use the secant method to solve equation (19) (in the elastic case) or (20) (in the viscoelastic case) for $a(t_i)$. To do this, we need to know $c(t_i)$ at each iteration. It is obtained using the secant method to solve the equation $K(c(t_i), t_i) = 0$ for $c(t_i)$, where the stress intensity factor $K(c, t)$ is given by (8). Note that we choose previous cohesive zone tip positions, $c(t_m)$, as initial approximations for $a(t_i)$ within the secant algorithm. The advantage of doing this is that we already know the stress history at these previous points since they were computed in the previous time steps. Note that $t_c(a_i)$ (the time instant when a_i became part of the cohesive zone) is unknown for cases when $a_i \neq c(t_m)$. Thus, we linearly interpolate $\delta_e(t_c(a_i), a_i)$ between $\delta_e(t_m, a_i)$ and $\delta_e(t_{m+1}, a_i)$ where $c_m < a_i < c_{m+1}$.

During implementation of the algorithm, we come across the step, i, where a_i will exceed c_{i-1}, and for decreasing cohesive zone length we will have $a_i > c_{i-1}$ in all the steps which follow. Thus, for these steps, only 1 previous value of c (namely c_{i-1}) can be taken as an initial approximation of a_i. To this end, we will modify the algorithm by fixing a_i and computing the corresponding t_i and c_i by solving equation (19) (in the elastic case) or (20) (in the viscoelastic case) (setting the crack tip opening displacement equal to the critical crack tip opening) and $K(c_i, t_i) = 0$ (setting the stress intensity factor to 0) respectively.

B. Numerical results

We used in our calculations the value $\delta_c = 1.13$ for the normalised critical crack tip opening, cf. Appendix.

Let $h = 1/5000$ be the step size in the time mesh. For $\beta = b/4 = 1$, we have 51 and 48 time steps before crack growth begins in the elastic and the viscoelastic cases, respectively, while $t_d = 0.0102$ for the elastic case and $t_d = 0.0096$ for the viscoelastic case.

The graphs in Figs. 10 and 11 show coordinates of the crack tip and the cohesive zone tip for both the elastic and viscoelastic cases.

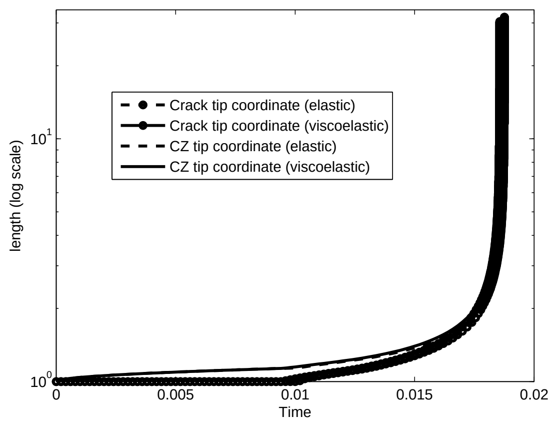

Fig. 10. Length vs. time for $b = 4$, $\beta = 1$

The graphs in Fig. 12 show the behaviour of the cohesive zone length with time. The graphs in Fig. 13 show the evolution of CZ tip coordinate in time for 3 cases of β.

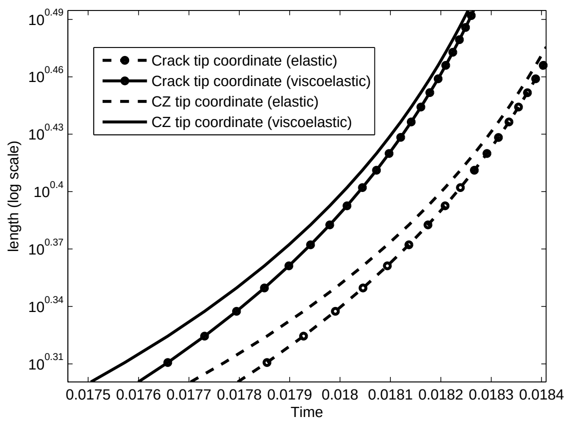

Fig. 11. Length vs. time for $b = 4$, $\beta = 1$

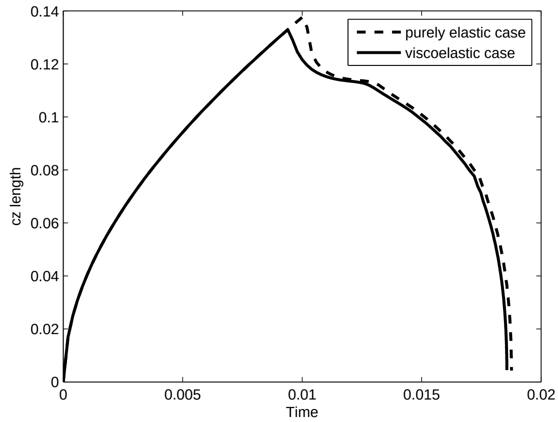

Fig. 12. CZ length vs. time for $b = 4$, $\beta = 1$

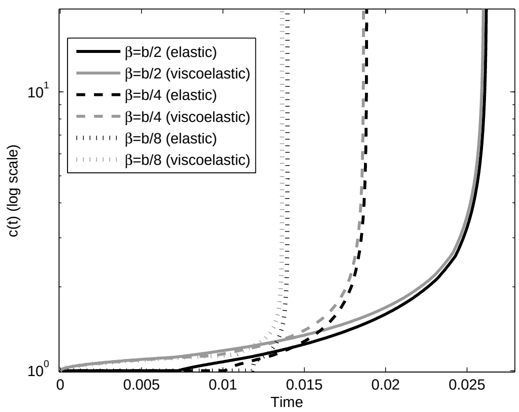

Fig. 13. CZ tip coordinate vs. time for $b = 4$

V. Conclusions

The solution converges as the mesh becomes finer.

For the stationary crack stage, $t < t_d$, the cohesive zone length is smaller for smaller β, for the same time instant. We can see from Figure 6 that the stress reaches a sharp maximum in coordinate at the cohesive zone tip and monotonically decreases with the distance from the tip. As expected, we have an increase, with time, of the crack tip opening. Moreover, as β becomes smaller, the crack tip opening increases more slowly with time. The obtained graph of the crack tip opening displacement for the viscoelastic case demonstrates that the crack opens at a higher rate than in the elastic case. As a consequence, the fracture delay time t_d is longer for the elastic case than for the viscoelastic one: for $b = 4$ and $\beta = 1$, we obtained $t_d = 0.0102$ for the elastic case and $t_d = 0.0096$ for the viscoelastic case.

For the growing crack stage, $t > t_d$, we can see from Figure 10, that the crack growth rate increases, while the cohesive zone length decreases with time. The time, when the cohesive zone length becomes 0 seems to coincide with the time when the crack length becomes infinite and can be associated with the complete fracture of the body. The graph of the cohesive zone length for the viscoelastic case indicates that the fracture time is slightly smaller than that for the purely elastic case. For example, for $b = 4$ and $\beta = 1$, the normalised fracture time is $t_r = 0.0188$ for the elastic case and $t_r = 0.0186$ for the viscoelastic one. It can be seen from Figure 13 that as β decreases, the fracture time also decreases.

Appendix

To give an idea on the parameter scales, we provide here some material parameters for PMMA from [8] (pages 655-657), [9], and [10]. Poisson's ratio $\nu = 0.35$; Young's modulus of elasticity $E_0 = 3100$ MPa; relaxation time $\eta/E_1 = 2.52 \cdot 10^4$ s; viscosity $\eta = 4.3 \cdot 10^7$ MPa s; critical crack tip opening: $\hat{\delta}_c = 0.0016$mm. Then by (18), $\delta_c = 1.13$ for $\hat{q}$ =5MPa.

Some experimental data on the static creep rupture under tensile stress for PMMA at the room temperature were reported in [11]. Fitting these data to the power-type durability curve $\hat{t}_\infty(\hat{\sigma}) = (\hat{\sigma}/\sigma_0)^{-b}$ will give values for b, σ_0, $\hat{t}_\infty(\hat{q})$, A_0 and A_1.

References

[1] Dugdale D.S., Yielding of steel sheets containing slits, *J. Mech. Phys. Solids*, Vol. 8, 100-104, 1960.

[2] Leonov M.Ya., Panasyuk V.V., Development of the smallest cracks in the solid, *Applied Mechanics (Prikladnaya Mekhanika)*, Vol. 5, No. 4, 391-401, 1959.

[3] Mikhailov S. E., Namestnikova I. V. History-sensitive accumulation rules for life-time prediction under variable loading, *Archive of Applied Mechanics*, Vol. 81, 1679-1696, 2011.

[4] Mikhailov S.E., Namestnikova I.V., Local and non-local approaches to creep crack initiation and propagation, *Proceedings of the 9th International Conference on the Mechanical Behaviour of Materials*, Geneva, Switzerland, 2003.

[5] Hakim L, Mikhailov S.E., Nonlinear Abel type integral equation in modelling creep crack propagation, *Integral Methods in Science and Engineering*: Computational and Analytic Aspects, editors: C. Constanda C. and P. Harris, Springer, 191-201, 2011.

[6] Muskhelishvili N.I., *Some Basic Problems of the Mathematical Theory of Elasticity*, Noordhoff International Publishing, The Netherlands, 1954.

[7] Rabotnov IU. N. *Elements of hereditary solid mechanics*, Mir Publishers, Russia, 1977.

[8] Mark J.E., *Polymer Data Handbook*, Oxford University Press, New York, 1999.

[9] Ro H.W., Ding Y, Lee H.J., Hines D.R., Jones R.L., Lin E.K., Karim A., Wu W.L., Soles C.L., Evidence for internal stresses induced by nanoimprint lithography, *Journal of Vacuum Science and Technology B*, Vol. 24, No. 6, 2006.

[10] Cotterell B., Fracture and life, *World Scientific*, Singapore, 2010.

[11] McKenna G.B., Crissman J. M., A Reduced Variable Approach to Relating Creep and Creep Rupture in PMMA, *MRS Proceedings*, Vol. 79, 333-343, 1986.

ISBN: 978-988-19251-0-7
ISSN: 2078-0958 (Print); ISSN: 2078-0966 (Online)